Journal of Hazardous Materials 203–204 (2012) 158–168

Contents lists available at SciVerse ScienceDirect

Journal of Hazardous Materials

journal homepage: www.elsevier.com/locate/jhazmat

Dry deposition of Mn, Zn, Cr, Cu and Pb in particles of sizes of 3 μm, 5.6 μm and 10 μm in central Taiwan

Guor-Cheng Fang*, Yi-Liang Huang, Jun-Han Huang, Chia-Kuan Liu

Department of Safety, Health and Environmental Engineering, HungKuang University, Sha-Lu, Taichung 433, Taiwan

ARTICLE INFO

Article history:
Received 25 July 2011
Received in revised form
30 November 2011
Accepted 30 November 2011
Available online 8 December 2011

Keywords:
Metallic elements
TSPs
Dry deposition
Dry deposition model

ABSTRACT

This investigates the concentrations of Mn, Zn, Cr, Cu, and Pb ambient air in total suspended particulates (TSPs) and dry deposition. The ratios of the calculated to measured dry deposition fluxes of ambient-air Mn, Zn, Cr, Cu and Pb at five characteristic sampling sites from 2009 to 2010 were determined using two dry deposition models. Experimental results demonstrate that the mean concentrations of metallic elements in TSPs and dry deposition were highest at the Quan-xing (industrial) sampling site, which is surrounded by various industrial factories and is in a severely polluted area. The mean seasonal concentrations of metallic elements in TSPs were highest in the winter and fall at all five sites. The analytical concentrations of metallic elements in fall and winter at these five sites were elevated in low winds. The Baklanov model yielded more accurate predictions concerning the dry deposition of metallic elements in ambient air when the sizes of the deposited particles were <5.6 μm, and the Noll and Fang model yielded better predictions when the sizes of the particles were >5.6 μm.

1. Introduction

Atmospheric particulate pollution has imposed a great burden on the terrestrial environment both regionally and globally [1]. Atmospheric deposition refers to the transfer of atmospheric pollutants to terrestrial and aquatic surfaces [2,3]. Heavy metals in the atmosphere, water, and soil are a great concern owing to their hazardous effect on human health [4].

Heavy metals are present in the atmosphere in increasing concentrations because of both anthropogenic and natural emissions [5]. Anthropogenic emissions are estimated to be three times greater than natural emissions [6]. Indeed, human activities (such as transportation and industrial production) discharge significant amounts of potentially toxic metals. Such elements become distributed in soil, air, surface dust and water. The metals accumulate because they are not easily degraded or decomposed in these environments [7,8].

Natural emissions are produced as crustal minerals undergo various processes, such as volcanism, erosion and the actions of surface winds, forest fires and oceans [9,10]. The largest anthropogenic source of Pb, Cu and As is traffic. Zn and Cr are industrial contaminants [11]. The aging and wear of heavy-duty vehicles release Zn from tires and Cu from brake linings [12]. However, metallurgical processes produce the greatest emissions of As, Cu and Zn [9,13]. The major source of the metallic element Cr is the combustion of coal [14,15].

Exposure to individual metallic elements can detrimentally affects humans in various ways. For example, prolonged exposure to Zn can cause arteriosclerosis, hypertension and heart disease, while Cr is carcinogenic and can lead to nasal septum perforation, asthma. Copper can cause nasal septum perforation, pulmonary granuloma, pulmonary interstitial fibrosis and lung cancer, while exposure to Pb can cause poisoning and anemia [16].

This investigates seasonal concentrations of metallic elements Mn, Zn, Cr, Cu and Pb in dry deposits and total suspended particulates (TSPs) at five characteristic sampling sites. It also identifies the size of particles for which the predictions made using various dry deposition models concerning the concentrations of Mn, Zn, Cr, Cu, and Pb in ambient air are the most accurate.

2. Method

2.1. Sampling program

Fig. 1 displays the five characteristic sampling sites. All samples were obtained in sampling period of 1380–1400 min. The sampling sites are similar to those in another [17].

The major sources of Mn, Zn, Cr, Cu, and Pb at the Bei-shi (suburban/coastal) sampling site were the Taichung Thermal Power Plant (TTPP) and a coastal industrial zone, both of which are located around 11 km southwest of the sampling site. The Taichung Science Park is southeast of this sampling site, and downtown is around

* Corresponding author. Tel.: +886 4 2631 8652x1111; fax: +886 4 2631 0744.
E-mail address: gcfang@sunrise.hk.edu.tw (G.-C. Fang).

0304-3894/$ – see front matter © 2011 Elsevier B.V. All rights reserved.
doi:10.1016/j.jhazmat.2011.11.098

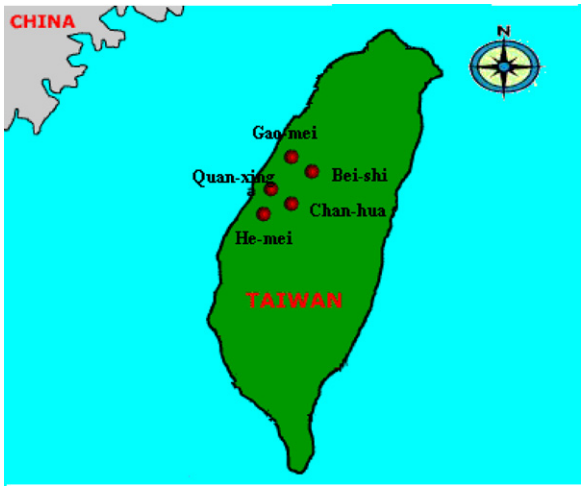

Fig. 1. Geographical location at five characteristic sampling sites in central Taiwan.

8 km away from this site. The major sources for the Chang-hua (downtown) sampling site were automobile emissions southeast of the site. A chemical plant is located around 15 km southwest of the site. Nearby sources of Mn, Zn, Cr, Cu, and Pb for the He-mei (residential) sampling site were transportation, agriculture, heating, and waste incineration. The major sources for the Quan-xing (industrial) sampling site were steel manufacturing, electronics factories, a plastics factory, chemical factories, basic metal manufacturing, and machinery manufacturing. Finally, the major sources for the Gao-mei (wetland) sampling site were the TTPP, located around 15 km to the south. A factory that burned coal and an expressway were also close to this sampling site.

2.2. Sampling program

2.2.1. PS-1 sampler

The PS-1 is a complete air sampling system, which is designed to collect suspended airborne particles (GMW High-Volume Air Sampler; Graseby-Andersen, country). The maximum size of the particles sampled in this investigation was around 100 μm. The flow rate through the sample was 200 L/min. A quartz filter with a diameter of 10.2 cm filtered the suspended particles. All filters were first conditioned for 24 h in an electric chamber at a humidity of 35 ± 5% and a temperature of 25 ± 5 °C prior to on and off weighing. Filters always transported and stored in a sealed CD box. The sampling device and procedures are similar to those used elsewhere another investigation [17].

2.2.2. Dry deposition plate

A DDP had a smooth horizontal, surrogate surface that provided a lower-bound estimate of the dry deposition flux. The DDP comprised of a plate with a smooth surface that was made of polyvinyl chloride (PVC) and was 21.5 cm long, 8.0 cm wide and 0.8 cm thick. The DDP also had a sharp, leading edge that pointed into the prevailing wind. The overhead projection films that were placed on the top surface of dry deposition plate (DDP) were used to collect the dry deposited pollutants. All of these overhead projection films were maintained at a relative humidity of 50% at 25 °C for more than 48 h. Before sampling, all of these films were weighed to a precision of 0.0001 g [17].

2.3. Chemical analysis

Samples were placed in an oven (25 °C) for 12 h before they were weighed. One quarter of each filter was cut away before the digestion process. The filters were then cut into thin pieces and placed in a Teflon cup. Next, 3 mL of hydrochloric acid (HCl) and 9 mL of nitrate (HNO_3) were mixed together and then poured into this cup. The samples were then heated at 50 °C on a hotplate for 2 h. After digestion on the hotplate, the samples were filtered. Following filtration, the sample solution was added to 0.2% HNO_3 to a yield a solution with final volume of 100 mL [35]. The samples were stored at 4 °C in a refrigerator for inductively coupled plasma–atomic emission spectrometer (ICP–AES) analysis. Concentrations of Mn, Zn, Cr, Cu, and Pb were determined. To analyze the metallic elements, ICP–AES analysis was carried out using a PerkinElmer Optima 2100 Plasma Emission Spectrometer. A 30 s delay and an argon gas plasma flow rate of 15 L/min were utilized. The nebulizer flow rate was set to 0.65 L/min, and the sample flow rate was set to 1.5 mL/min.

2.4. Quality control

Blank test background contamination was determined using operational blanks (unexposed projection film and a quartz filter) that were processed with the field samples. The field blanks were exposed in the field when the sampling box was opened to remove and replace the filters. Background contamination by metallic elements was accounted for by subtracting the field blank values from the concentrations. Field blank values were extremely low – generally below or close to the method detection limits. Therefore, in this investigation, background contamination was insignificant and so disregarded. The blank test results were 0.30, 0.32, 0.20, 0.19 and 0.22 μg for Mn, Zn, Cr, Cu, and Pb, respectively.

2.5. Dry deposition models

Atmospheric particles with aerodynamic diameters <10 μm (PM_{10}) have recently been closely investigated as they are easily inhaled and deposited in the respiratory system [18]. Relevant investigations have established that PM_{10} affects the incidence and severity of respiratory diseases [19,20]. Additionally, coarse particles may be more strongly related to respiratory health effects while the fine fraction tends to be more strongly associated with cardiovascular disease and mortality [21]. Therefore, V_d was calculated using 3 μm, 3–5.6 μm and 10 μm particles, using two dry deposition models, for all of the metallic elements in this investigation. The results in this investigation are then compared with measured dry deposition fluxes of all metals at the five characteristic sampling sites.

The two dry deposition models are as follows.

2.5.1. Baklanov and Sorensen's model

Baklanov and Sorensen [22] developed deposition models for computing long-range deposition. They defined dry deposition velocity as the inverse of a sum of resistances r_a, r_b and r_c in three sequential layers [23,24]. The model has the following form for gaseous pollutants.

$$V_d = (r_a + r_b + r_c)^{-1},$$

where r_a is the aerodynamic resistance; r_b represents the resistance to penetration across the atmospheric laminar sublayer, and r_c is the resistance associated with direct pollutant–surface interaction.

Baklanov and Sorensen [22] suggested that the transfer resistance, r_c, is negligible for particles, since when it encounters a surface, a particle is considered to be deposited. For particles, Seinfield suggested using the term $r_a r_b v_g$ rather than r_c.

Table 1
Meteorological conditions and metallic elements (Mn, Zn, Cr, Cu and Pb) in total suspended particulates (TSP) and dry deposition at five characteristic sampling sites during year 2009–2010.

	Bei-shi (suburban/coastal) ($N=60$)		Chang-hua (downtown) ($N=60$)		He-mei (residential) ($N=60$)		Quan-xing (industrial) ($N=60$)		Gao-mei (wetland) ($N=60$)	
	TSP (ng/m^3)	Flux (ng/m^2 min)	TSP (ng/m^3)	Flux (ng/m^2 min)	TSP (ng/m^3)	Flux (ng/m^2 min)	TSP (ng/m^3)	Flux (ng/m^2 min)	TSP (ng/m^3)	Flux (ng/m^2 min)
Spring										
Mn	39.0 ± 5.65	17.6 ± 3.45	55.0 ± 13.6	14.5 ± 3.15	62.7 ± 15.4	14.8 ± 3.91	83.7 ± 17.3	19.2 ± 3.84	28.2 ± 7.36	15.8 ± 4.12
Zn	103 ± 22.4	34.5 ± 5.26	93.3 ± 17.3	35.3 ± 6.98	96.8 ± 22.0	36.7 ± 9.68	107 ± 21.4	44.6 ± 18.0	77.8 ± 21.0	35.7 ± 9.56
Cr	27.2 ± 6.2	17.7 ± 4.72	39.3 ± 5.55	19.5 ± 6.22	28.2 ± 7.4	19.2 ± 5.17	36.9 ± 7.5	19.6 ± 3.83	21.5 ± 6.01	17.1 ± 4.76
Cu	84.7 ± 28.6	38.0 ± 4.52	70.6 ± 19.5	30.3 ± 3.59	76.9 ± 25.6	33.6 ± 4.30	105 ± 28.2	44.4 ± 10.7	64.3 ± 16.3	24.9 ± 2.6
Pb	30.7 ± 16.6	35.3 ± 5.33	27.8 ± 5.33	28.1 ± 4.25	32.4 ± 6.55	31.3 ± 5.17	40.5 ± 10.9	41.4 ± 9.26	25.7 ± 5.7	24.5 ± 4.46
Temp (°C)	20.6		20.8		20.8		20.7		21.0	
RH (%)	84		75		78		81		80	
WS (m/s)	1.7		1.6		2.4		3.2		2.5	
PWD	SE		SSE		SE		SE		SEE	
Summer										
Mn	32.9 ± 4.81	14.6 ± 2.11	50.42 ± 13.2	13.3 ± 3.31	53.8 ± 17.3	12.7 ± 3.72	67.8 ± 19.2	15.4 ± 3.99	21.4 ± 8.63	11.9 ± 4.33
Zn	91.5 ± 11.0	29.6 ± 4.20	76.0 ± 20.2	30.3 ± 7.68	82.2 ± 27.6	30.3 ± 10.1	95.0 ± 21.1	27.4 ± 4.81	60.4 ± 25.2	30.1 ± 12.0
Cr	19.7 ± 5.07	15.5 ± 3.61	32.1 ± 4.31	15.7 ± 3.95	21.5 ± 6.75	15.5 ± 4.62	28.7 ± 6.15	16.3 ± 2.36	16.2 ± 6.02	14.6 ± 5.41
Cu	80.44 ± 26.4	32.7 ± 6.55	64.6 ± 16.4	26.0 ± 5.21	71.9 ± 19.1	29.0 ± 6.25	101 ± 21.9	41.1 ± 6.86	50.4 ± 17.8	23.3 ± 5.20
Pb	27.3 ± 6.76	29.7 ± 3.54	23.8 ± 5.27	23.6 ± 2.82	26.5 ± 6.3	26.3 ± 3.57	33.2 ± 6.08	33.9 ± 4.91	21.1 ± 5.22	21.9 ± 3.29
Temp (°C)	27.4		27.8		27.5		27.1		27.6	
RH (%)	81		75		79		83		80	
WS (m/s)	2.5		2.4		2.6		2.8		2.4	
PWD	SW		SW		SW		SW		SW	
Fall										
Mn	34.3 ± 11.5	15.6 ± 3.79	53.87 ± 11.2	14.5 ± 3.13	60.1 ± 16.6	14.0 ± 4.53	79.7 ± 18.4	18.3 ± 4.49	23.0 ± 7.43	12.4 ± 3.22
Zn	106 ± 46.8	37.4 ± 9.87	90.4 ± 23.2	35.4 ± 8.72	89.9 ± 28.3	34.0 ± 7.84	111 ± 31.9	33.7 ± 4.96	63.6 ± 19.8	31.4 ± 10.0
Cr	25.4 ± 7.48	17.1 ± 4.33	27.4 ± 7.08	16.5 ± 2.48	21.9 ± 7.37	16.5 ± 4.05	29.2 ± 4.83	20.8 ± 5.77	17.4 ± 5.58	15.3 ± 6.16
Cu	105.5 ± 20.7	49.8 ± 13.5	69.3 ± 22.9	44.6 ± 20.0	88.0 ± 17.8	49.4 ± 23.0	117 ± 89.3	51.8 ± 18.0	62.8 ± 15.0	42.2 ± 14.0
Pb	42.7 ± 12.3	46.4 ± 9.78	34.5 ± 22.5	41.8 ± 15.2	38.0 ± 24.8	46.5 ± 17.7	45.7 ± 13.1	47.8 ± 15.5	30.0 ± 17.0	45.2 ± 12.7
Temp (°C)	27.9		29.0		28.8		28.5		27.9	
RH (%)	71		71		73		75		76	
WS (m/s)	1.9		1.7		2.1		2.5		2.0	
PWD	SW		SW		S		SE		SE	
Winter										
Mn	39.6 ± 8.7	16.4 ± 2.31	62.42 ± 13.05	17.8 ± 3.21	64.1 ± 9.62	14.9 ± 3.87	95.6 ± 5.94	19.5 ± 3.41	27.5 ± 3.87	16.0 ± 3.67
Zn	115 ± 29.8	35.7 ± 5.2	102 ± 13.8	39.1 ± 7.55	107 ± 10.6	39.1 ± 3.59	124.3 ± 17.8	36.7 ± 4.71	74.7 ± 4.37	39.1 ± 6.93
Cr	21.8 ± 6.66	17.1 ± 4.33	33.1 ± 6.42	18.6 ± 3.61	22.5 ± 10.1	18.0 ± 4.81	32.9 ± 6.02	17.9 ± 3.18	18.9 ± 4.96	19.5 ± 5.21
Cu	88.7 ± 24.5	49.8 ± 13.5	80.5 ± 17.1	30.0 ± 6.71	78.7 ± 23.1	33.4 ± 7.55	117 ± 43.5	44.6 ± 11.7	68.2 ± 16.5	29.2 ± 7.69
Pb	34.9 ± 6.7	46.4 ± 9.78	29.2 ± 5.89	32.5 ± 3.97	30.8 ± 6.04	36.1 ± 4.99	37.2 ± 8.76	47.4 ± 9.21	22.1 ± 9.00	30.6 ± 4.93
Temp (°C)	20.1		21.1		21.2		21.2		21.2	
RH (%)	72		69		72		75		74	
WS (m/s)	1.4		1.3		1.7		2.1		1.8	
PWD	SE		SE		SE		SE		SE	
Average										
Mn	36.3 ± 8.44	16.0 ± 3.13	55.3 ± 13.2	15.0 ± 3.55	60.1 ± 15.3	14.1 ± 4.02	81.9 ± 18.4	18.1 ± 4.2	24.8 ± 7.5	13.9 ± 4.22
Zn	104 ± 30.9	34.3 ± 7.05	90.2 ± 20.9	35.0 ± 8.22	93.7 ± 24.6	34.9 ± 8.68	109 ± 25.5	35.4 ± 11.4	68.8 ± 20.3	34.1 ± 10.4
Cr	23.5 ± 6.92	17.5 ± 4.41	32.9 ± 7.18	17.6 ± 4.41	23.5 ± 8.24	17.2 ± 4.77	31.8 ± 6.88	18.7 ± 4.26	18.3 ± 5.89	16.7 ± 5.74
Cu	90.0 ± 26.9	39.6 ± 10.8	71.1 ± 19.6	32.8 ± 13.1	78.9 ± 21.8	36.4 ± 14.9	110 ± 52.5	45.5 ± 12.8	60.7 ± 17	30.4 ± 11.8
Pb	33.9 ± 12.5	38.1 ± 8.9	28.8 ± 12.7	31.5 ± 10.6	31.9 ± 14.04	35.1 ± 12.3	39.2 ± 10.9	42.5 ± 11.7	25.1 ± 10.8	30.8 ± 11.9
Temp (°C)	24.0		24.7		24.5		24.4		24.4	
RH (%)	77		72		75		78		77	
WS (m/s)	1.9		1.8		2.2		2.6		2.2	
PWD	S		S		SE		SE		SE	

The above formula for the dry deposition velocity of particles includes a term that is determined by the sedimentation/gravitational settling of particles:

$$V_d = (r_a + r_b + r_a r_b v_g)^{-1} + v_g,$$

where v_g is the gravitational settling velocity.

Aerodynamic resistance, r_a, depends on meteorological parameters such as wind speed, atmospheric stability and surface roughness) as follows.

$$r_a = \frac{[\ln(Z_s/Z_o) - \Psi_c]}{k u_*},$$

where Z_s is the height of first reference level and L is the Monin–Obuhkov length.

Surface layer resistance, r_b, depends on the parameters of diffusion across a laminar sublayer. Therefore, it depends on molecular rather than turbulent properties. Therefore, the surface layer resistance for particles differs from that for gases. According to Zannetti [27], the surface layer resistance for particles can be expressed as a function of the Schmidt number, $S_c = \nu/D$, and the Stokes number, St:

$$r_b = (S_c^{-2/3} + 10^{-3/St})^{-1} u_*^{-1}$$

The airflow around a falling particle with a diameter of under approximately 3.5 μm can be regarded as laminar. However, for larger particles, Stokes law does not hold; additionally, an iterative procedure must be used to solve the equation for the terminal

Table 2
Metallic elements concentrations study in TSP for different cities during 2000–2010.

Year	City	Character	Metal (ng/m^3)					Reference
			Mn	Zn	Cr	Cu	Pb	
TSP								
2000	Tokyo(Japan)	Urban	–	298.7	6.1	30.2	124.7	Var et al. [30]
2001	Ho Chi Minh (Vietnam)	Urban	–	203	8.6	1.3	146	Hien et al. [31]
2002	Taejon (Korea)	Industrial	50.3	240	25.1	–	243	Kim et al. [33]
2003	Taichung (Taiwan)	Urban	–	395.3	29.3	198.6	573.6	Fang et al. [32]
2004	Delhi (India)	Urban	–	–	104	–	380	Khillare et al. [34]
2005	Beijing (China)	Urban	374	1214	29	178	690	Okuda et al. [28]
2006	Beijing (China)	Urban	296	1087	23	157	693	Okuda et al. [28]
2007	Hong Kong (China)	Urban	39.5	50.8	13.9	13.9	55	Lee and co-workers [29]
2010	Bei-shi (Taiwan)	Suburban/coastal	36.3	104	23.5	90	33.9	This study
2010	Chang-hua (Taiwan)	Downtown	55.3	90.2	32.9	71.1	28.8	This study
2010	He-mei (Taiwan)	Residential	60.1	93.7	23.5	78.9	31.9	This study
2010	Quan-xing (Taiwan)	Industrial	81.9	109	31.8	110	39.2	This study
2010	Gao-mei (Taiwan)	Wetland	24.8	68.8	18.3	60.7	25.1	This study

settling velocity in the turbulent regime, and this was developed by Näslund and Thaning [25]:

$$\frac{Dw_p}{dt} = (w - wp)f(V) - \beta g,$$

$$f(V) = \frac{3\rho V C_d}{8 r \rho_p},$$

$$V = ((u - u_p)^2 + (v - v_p)^2 + (w - w_p)^2)^{1/2},$$

$$C_d = \frac{24}{Re[1 + 0.173(Re)^{0.657}]} + \frac{0.413}{(1 + 16300(Re)^{-1.09})},$$

where V denotes the relative velocity of the particles; u, v, w, u_p, v_p and w_p are the components of the velocities of the air and particles; β is the buoyancy effect parameter, $\beta = (\rho_p - \rho)/\rho_p$; C_d is the drag coefficient in the static state; and Re is the Reynolds number, $Re = 2Vr/v$.

2.5.2. Noll and Fang's model

Noll and Fang's dry deposition model yields the following deposition velocities of atmospheric particles [26].

$$V_d = V_{st} + 1.12U^* \chi \exp\left(\frac{-30.36}{D_p}\right)$$

where V_d is particle settling velocity (cm/s), U^* denotes (cm/s), and D_p denotes particle diameter (μm).

Two meteorological parameters that affect atmospheric turbulence are frictional velocity U^* and surface roughness Z_0. The relationship between these parameters under near-natural atmospheric stability conditions is

$$U = \left(\frac{U^*}{\kappa}\right) \times \ln\left[\frac{(Z-d)}{Z_0}\right]$$

where U denotes the measured average wind speed at height Z (m/s); Z denotes measured height above ground (m); k is von Karmon's constant (0.4); d denotes displacement (m); and Z_0 denotes surface roughness height (m).

3. Results and discussion

Table 1 presents the meteorological conditions and Mn, Zn, Cr, Cu, and Pb concentrations in TSPs and dry deposition at the five characteristic sampling sites in 2009–2010.

The meteorological parameters were measured using a Watch Dog Model 525 (Spectrum Technologies, Inc., Taichung County, Taiwan). The sampling heights at which the wind speeds were measured at Quan-xing (industrial), Gao-mei (wetland), He-mei (residential), Chang-hua (downtown) and Bei-shi (suburban/coastal) sampling sites were 12 m, 12 m, 7 m, 7 m and 12 m, respectively.

Spring lasts from February to April; summer lasts from May to July; fall lasts from August to October, and winter lasts from November to January.

The mean of the four seasonal concentrations of each of the metallic elements Mn, Zn, Cr, Cu and Pb in TSPs (ng/m^3) and dry deposits (ng/m^2 min) was highest at the Quan-xing (industrial) sampling site. In TSPs (ng/m^3), it was lowest at the Gao-mei (wetland) sampling site. The average concentrations of Cr, Cu and Pb in dry deposits (ng/m^2 min) in the spring were lowest at the Gao-mei (wetland) sampling site. However, the concentrations of Mn and Zn in the spring were lowest at the Bei-shi (suburban/coastal) and Chang-hua (downtown) sampling sites.

The average concentrations of Mn, Cr, Cu and Pb in dry deposits (ng/m^2 min) in the summer were lowest at the Gao-mei (wetland) sampling site. However, that of Zn was lowest at the Quan-xing (industrial) sampling site.

The average concentrations of Mn, Zn, Cr, Cu and Pb in dry deposits (ng/m^2 min) in the fall were lowest at the Gao-mei (wetland) sampling site. Those of Mn, Cu and Pb in the winter were lowest at the Gao-mei (wetland) sampling site, while those of Zn and Cr were lowest at the Bei-shi (suburban/coastal) sampling site.

The results reveal that the seasonal concentrations of dry deposited metallic elements were highest in industrial areas and zones with heavy traffic. The main sources for the Gao-mei (wetland) sampling site were the Taichung thermal power plant (TTPP) and the combustion of fossil fuel. Additionally, it may be subject to an far source from which pollution is transported over a long distance when a northwesterly wind blows from mainland China. For the Quan-xing (industrial) sampling site, the nearby sources were the steel industry, electronic industry, plastic industry, chemical industry, metal manufacturing, machinery manufacturing, and petroleum and coal production. Finally, the main sources for the Bei-shi (suburban/coastal) and Chang-hua (downtown) sampling sites were the nearby science park, fossil fuel combustion and transportation.

The seasonal variations in the concentrations of the metallic pollutants were affected not only by nearby sources of pollution but also by the distance to these sources. Air emissions from industrial activities may even affect residential areas at remote distances from industrial sectors [39]. Generally speaking, a low mixed layer will make the suspended particulate concentrations spread uneasily and a weak rainfall usually will not be enough to easily remove suspended particulate concentrations from the atmosphere. PM_{10} particles were slightly increased in the winter season of Taiwan

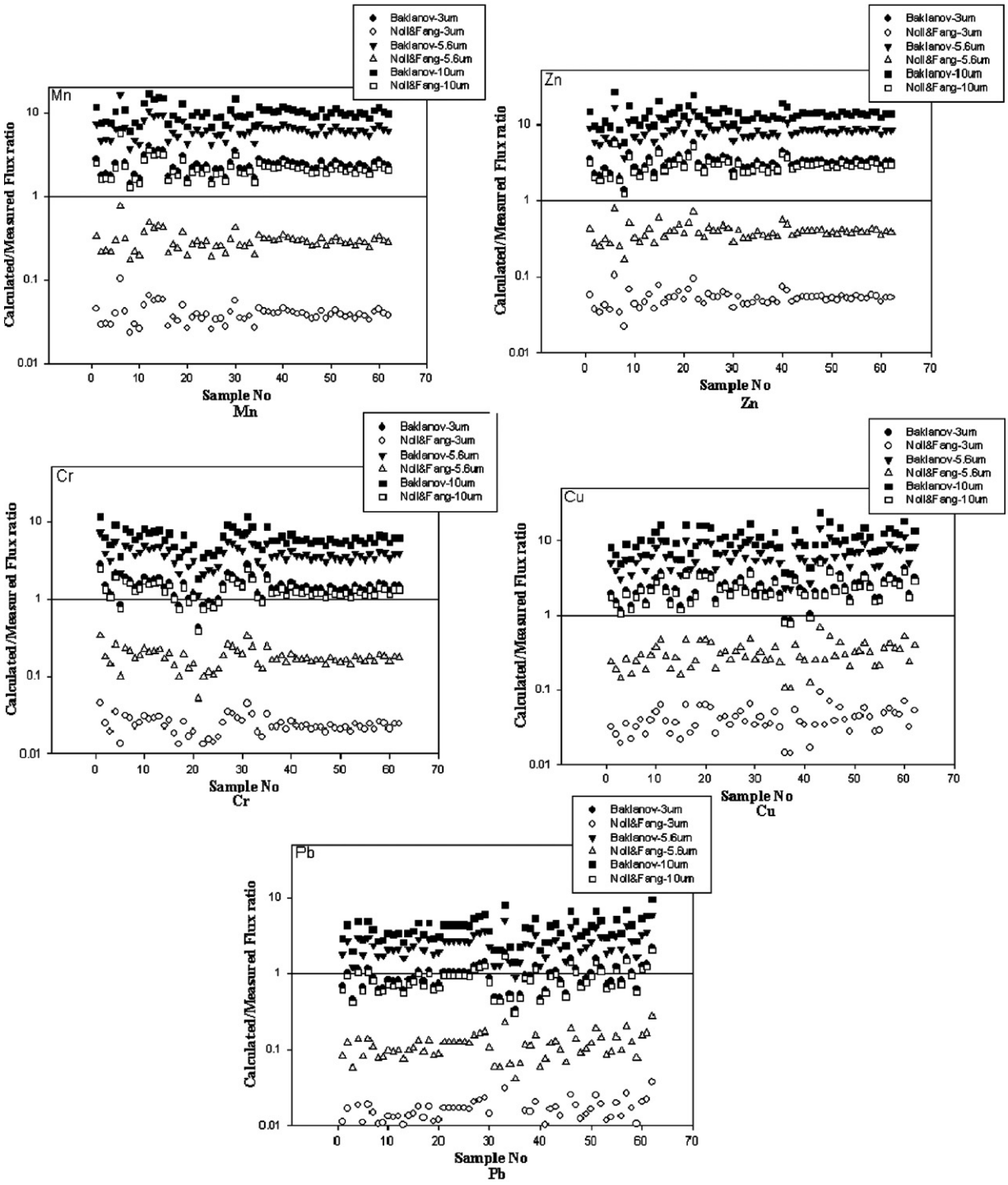

Fig. 2. Measured flux ratios for Mn, Zn, Cr, Cu, and Pb at the Bei-shi (suburban/coastal) sampling site using different dry deposition models for particle sizes 3 μm, 5.6 μm, and 10 μm.

[38]. Additionally, seasonal differences in the metal concentrations may be due to differences in wind directions with some winds passing through industry or traffic areas [39]. Thus, the geology, sampling height and meteorological conditions – especially in the autumn and fall strongly affected the seasonal variations in the concentrations of metallic pollutants. Seasonally, concentrations were found to be lowest during the monsoon season (July–September) [37]. Moreover, the average wind speed was lowest in the autumn and winter seasons of this study. This fact may have been chiefly responsible for the high average concentrations of the metallic elements in these seasons. In addition, previous study also indicated that the doubled concentrations in winter were likely caused by coal combustion (Pb) and biomass burning (K), but also by a lower mixing layer height [36]. Therefore, all the above factors were also responsible for the high metallic elements concentrations in the winter season of this study.

Table 2 presents the concentrations of metallic elements in TSPs in different cities from 1000 to 2010). The highest average concentration of Mn in TSP was found in Quan-xing (Taiwan, average 81.9 ng/m^3) and the lowest was found in Gao-mei (Taiwan, average

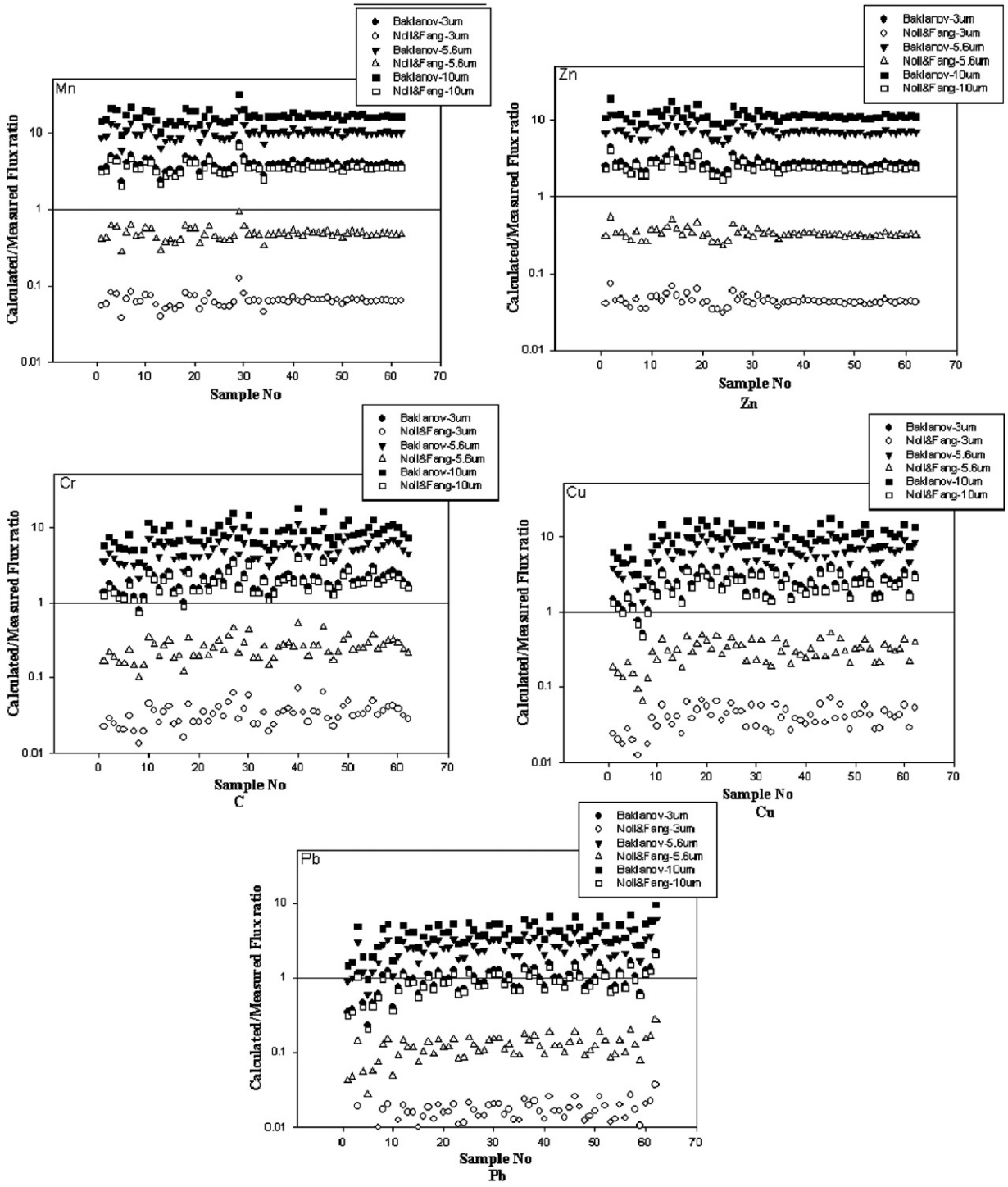

Fig. 3. Measured flux ratios for Mn, Zn, Cr, Cu and Pb at the Chang-hua (downtown) sampling site with different dry deposition models for particle sizes 3 μm, 5.6 μm, and 10 μm.

24.8 ng/m^3). The highest concentration of Zn in TSP was found in Beijing (China, average 1214 ng/m^3) [28] and the lowest was found in Hong-Kong (China, average 50.8 ng/m^3) [29]. The highest average concentration of Cr in TSP was found in Delhi (India, average 104 ng/m^3) [34] and the lowest was found in Ho Chi Minh (Vietnam, average 8.6 ng/m^3) [31]. The highest concentration of Cu was found in Taichung (Taiwan, average 198.6 ng/m^3) [32] and the lowest was found in Ho Chi Minh (Vietnam, average 1.3 ng/m^3) [31]. The highest concentration of Pb in TSP was found in Beijing (China, average 693 ng/m^3) [28] and the lowest was found in Gao-mei (Taiwan, average 25.1 ng/m^3).

Fig. 2 plots the measured flux ratios for Mn, Zn, Cr, Cu, and Pb at the Bei-shi (suburban/coastal) sampling site using various dry deposition models for particles of size 3 μm, 5.6 μm, and 10 μm. According to the Baklanov model, the average measured Mn flux ratios for particles of size 3 μm, 5.6 μm, and 10 μm were 2.45, 6.39, and 10.3, respectively. The average measured Zn flux ratios for particles of size 3 μm, 5.6 μm, and 10 μm were 3.21, 8.38 and 13.4,

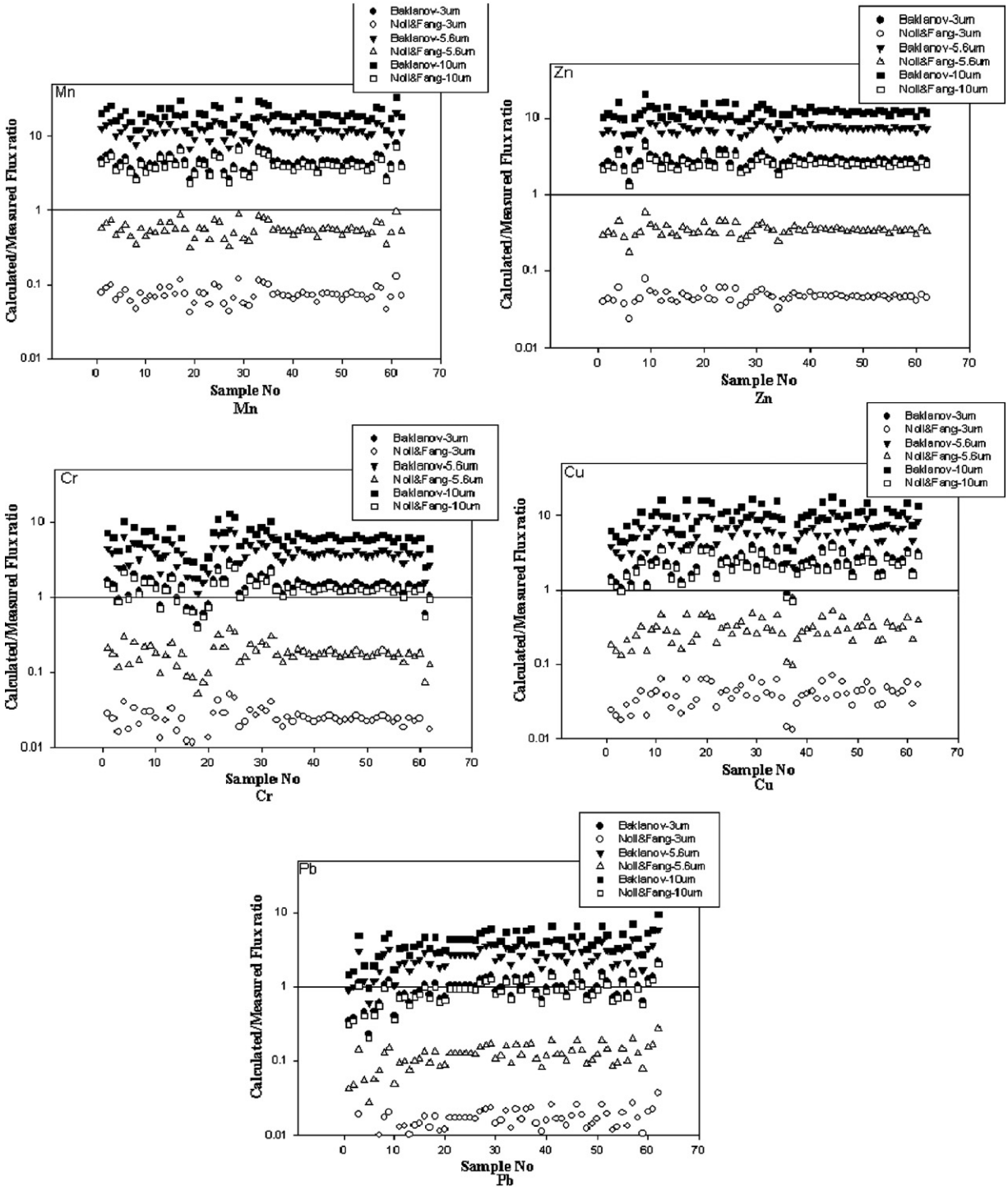

Fig. 4. Measured flux ratios for Mn, Zn, Cr, Cu, and Pb at the He-mei (residential) sampling site by the different dry deposition models for various particle sizes 3 μm, 5.6 μm, and 10 μm.

respectively. The average measured flux ratios of Cr for particles of size 3 μm, 5.6 μm and 10 μm were 1.45, 3.79 and 6.08, respectively. Those of Cu were 2.51, 6.56, and 10.5, respectively. Finally, those of Pb measured flux ratios for 3 μm, 5.6 μm, and 10 μm were 0.96, 2.51, and 4.03, respectively.

According to the Noll and Fang model, the average measured Mn flux ratios for particles of size 3 μm, 5.6 μm, and 10 μm were 0.04, 0.29, and 2.17, respectively. Those of Zn were 0.05, 0.39, and 2.85, respectively. Those of Cr were 0.02, 0.17, and 1.29, respectively. Those of Cu were 0.04, 0.30, and 2.23, respectively. Finally, those of Pb were 0.02, 0.12, and 0.85, respectively.

Fig. 3 plots measured flux ratios of Mn, Zn, Cr, Cu and Pb at the Chang-hua (downtown) sampling site obtained using different dry deposition models for particles of size 3 μm, 5.6 μm, and 10 μm. According to the Baklanov model, the average measured Mn flux ratios for particles of size 3 μm, 5.6 μm, and 10 μm were 3.93, 10.3, and 16.5, respectively. Those of Zn were 2.74, 7.15, and 11.5, respectively. Those of Cr were 2.09, 5.44, and 8.73, respectively. Those of

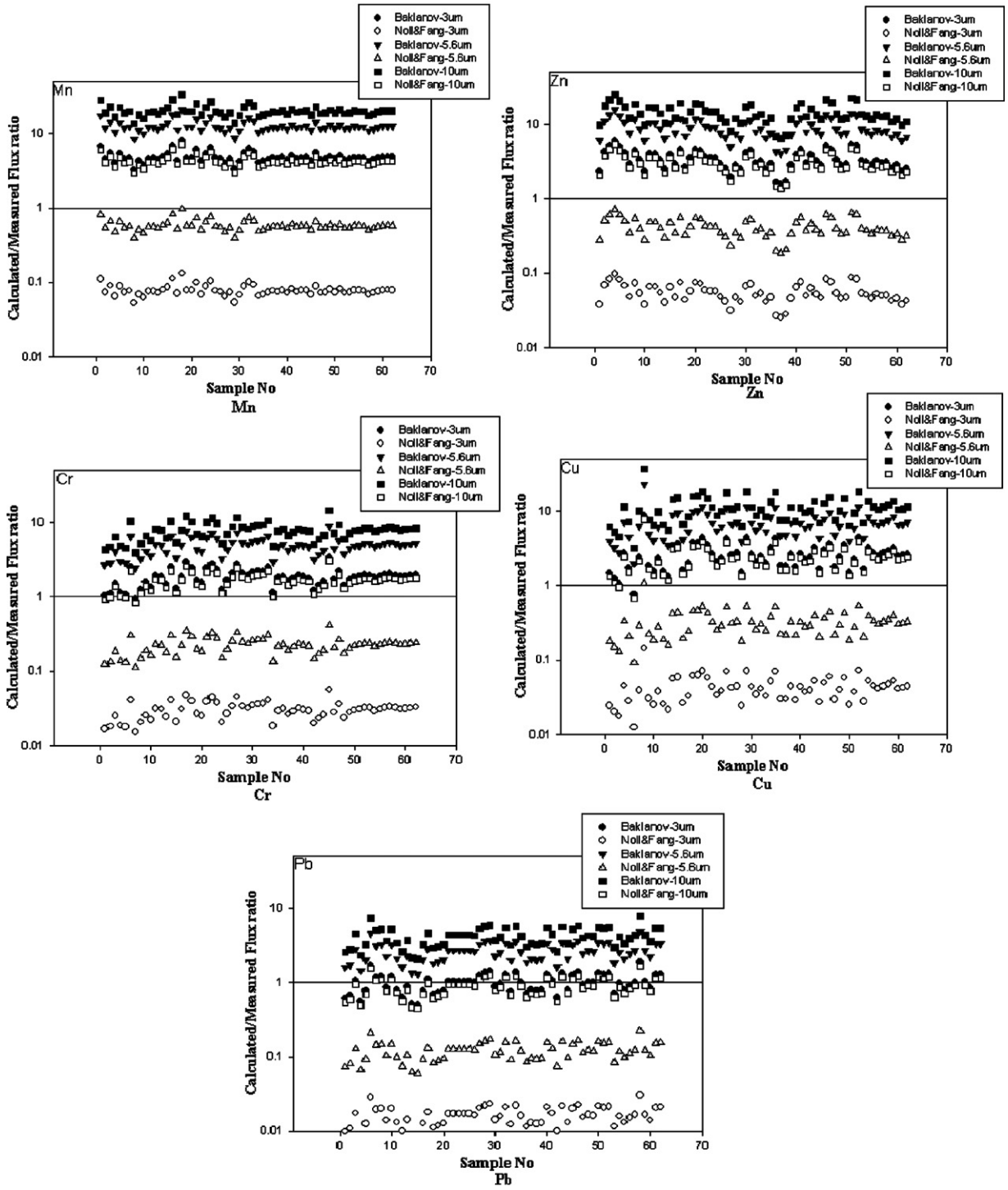

Fig. 5. Measured flux ratios for Mn, Zn, Cr, Cu, and Pb at the Quan-xing (industrial) sampling site by different dry deposition models at particle sizes of 3 μm, 5.6 μm, and 10 μm.

Cu were 2.47, 6.45, and 10.3, respectively. Finally, those of Pb were 0.99, 2.61, and 4.18, respectively.

According to the Noll and Fang model, the average measured Mn flux ratios for particles of size 3 μm, 5.6 μm, and 10 μm were 0.06, 0.47, and 3.49, respectively. Those of Zn were 0.05, 0.33, and 2.43, respectively. Those of Cr were 0.04, 0.29, and 2.19, respectively. Those of Cu were 0.04, 0.30 and 2.23, respectively. Finally, those of Pb were 0.02, 0.12, and 0.89, respectively.

Fig. 4 plots the measured flux ratios of Mn, Zn, Cr, Cu, and Pb at the He-mei (residential) sampling site obtained using the different dry deposition models for particles of size 3 μm, 5.6 μm, and 10 μm. The average measured Mn flux ratios obtained using the Baklanov model were 4.61, 12.0, and 19.3, respectively. Those of Zn were 2.85, 7.43, and 11.9, respectively. Those of Cr were 1.48, 3.84, and 6.17, respectively. Those of Cu were 2.45, 6.40, and 10.3, respectively. Finally, those of Pb were 1, 2.61, and 4.19, respectively.

Based on the Noll and Fang model, the average measured Mn flux ratios for particles of size 3 μm, 5.6 μm, and 10 μm were 0.07, 0.56, and 4.09, respectively. Those of Zn were 0.05, 0.34, and 2.53, respectively. Those of Cr were 0.02, 0.18, and 1.31, respectively.

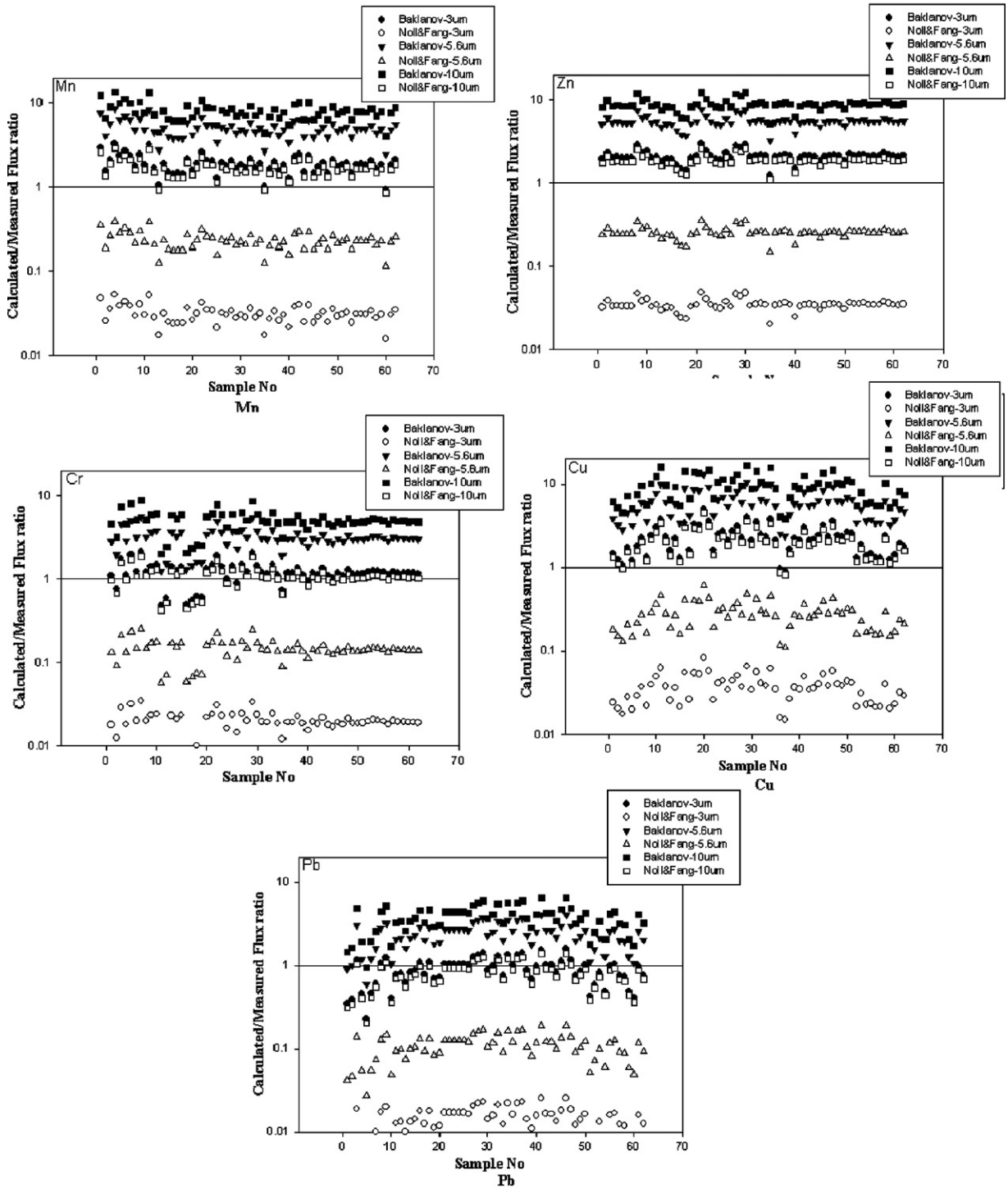

Fig. 6. Measured flux ratios for Mn, Zn, Cr, Cu and Pb at the Gao-mei (wetland) sampling site by different dry deposition models for particle sizes 3 μm, 5.6 μm, and 10 μm.

Those of Cu were 0.04, 0.29, and 2.18, respectively. Finally, those of Pb were 0.02, 0.12, and 0.89, respectively.

Fig. 5 plots the measured flux ratios of Mn, Zn, Cr, Cu, and Pb at the Quan-xing (industrial) sampling site obtained using different dry deposition models for particles of size 3 μm, 5.6 μm, and 10 μm. Based on the Baklanov model, average measured Mn flux ratios were 4.82, 12.6, and 20.2, respectively. Those of Zn were 3.41, 8.90 and 14.3, respectively. Those of Cr were 1.86, 4.85, and 7.78, respectively. Those of Cu were 2.66, 6.93, and 11.1, respectively. Finally, those of Pb were 1.01, 2.63 and 4.22, respectively.

According to the Noll and Fang model, the average measured Mn flux ratios for particles of size 3 μm, 5.6 μm, and 10 μm were 0.08, 0.58, and 4.28, respectively. Those of Zn were 0.06, 0.41, and 3.03, respectively. Those of Cr were 0.03, 0.22, and 1.65, respectively. Those of Cu were 0.04, 0.32, and 2.36, respectively. Finally, those of Pb were 0.02, 0.12, and 0.89, respectively.

Fig. 6 plots the measured flux ratios of Mn, Zn, Cr, Cu and Pb at the Gao-mei (wetland) sampling site obtained using different dry deposition models for particles of size 3 μm, 5.6 μm, and 10 μm. Based on the Baklanov model, the average measured Mn flux ratios

for particles of size 3 μm, 5.6 μm, and 10 μm were 1.90, 4.96, and 7.95, respectively. Those of Zn were 2.11, 5.52, and 8.85, respectively. Those of Cr were 1.20, 3.13, and 5.02, respectively. Those of Cu were 2.27, 5.93, and 9.51, respectively. Finally, those of Pb were 0.91, 2.36 and 3.78, respectively.

According to the Noll and Fang model, the average measured Mn flux ratios for particles of size 3 μm, 5.6 μm, and 10 μm were 0.03, 0.23, and 1.69, respectively. Those of Zn measured were 0.03, 0.26, and 1.88, respectively. Those of Cr were 0.02, 0.14, and 1.06, respectively. Those of Cu were 0.04, 0.27, and 2.02, respectively. Finally, those of Pb were 0.02, 0.11, and 0.81, respectively.

Analytical results reveal that the Noll and Fang model yielded better predictions for the dry deposition of Mn, Zn, Cr, Cu and Pb in ambient air when the particle size exceeded 5.6 μm, whereas the Baklanov model yielded better predictions for dry deposition when the particle size was less than 5.6 μm.

4. Conclusions

The results of this investigation support the following conclusions. Average seasonal concentrations of Mn, Zn, Cr, Cu, and Pb in TSPs and dry deposits were highest in the fall and winter and lowest in the summer at all five characteristic sampling sites. In addition, the average concentrations of Mn, Zn, Cr, Cu, and Pb in TSPs were highest at the Quan-xing (industrial) site, and lowest concentrations at the Gao-mei (wetland) site. However, the average concentrations of dry deposited Mn, Zn, Cr, Cu and Pb were highest at the Quan-xing (industrial) site, because the Quan-xing (industrial) site is in an industrial area in which many industrial processes take place. Furthermore, for 3 μm particles, the Baklanov model overestimated the dry deposition of Mn, Zn, Cr, and Cu from ambient air at the five characteristic sampling sites. For 10 μm particles, the Noll and Fang model overestimated the dry deposition of Mn, Zn, Cr, and Cu from ambient air at the five characteristic sampling sites. Finally, the Baklanov model underestimated the dry deposition of Pb in 3 μm particles from ambient air at the five characteristic sampling sites. However, the Noll and Fang model underestimated the dry deposition of Pb in 10 μm particles from ambient air at the five characteristic sampling sites.

Acknowledgment

The authors gratefully acknowledge the National Science Council of the ROC (Taiwan) for financial support under project no. NSC 99-2221-E-241-006-MY3.

References

[1] C. Venkataraman, G. Habib, A. Eiguren-Fernandez, A.H. Miguel, S.K. Friedlander, Residential biofuels in South Asia: carbonaceous aerosol emissions and climate impacts, Science 307 (2005) 1454–1456.
[2] R.A. Valigura, T.L. Winston, R.S. Artz, B.B. Hicks, Atmospheric nutrient input to coastal areas reducing the uncertainties, in: NOAA Coastal Ocean Program Decision Analysis Series No. 9, NOAA Coastal Ocean Office, Silver Spring, MD, 1996, 24 pp. + 4 appendices.
[3] C.C. Chu, G.C. Fang, J.C. Chen, I.L. Yang, Dry deposition study by using dry deposition plate and water surface sampler in Shalu, central Taiwan, Environ. Monitor. Assess. 146 (2008) 1441–1451.
[4] H. Van Malderen, S. Hoornaert, R. Van Grieken, Identification of individual aerosol particles containing Cr, Pb and Zn above the North Sea, Environ. Sci. Technol. 30 (1996) 489–498.
[5] K. Suzuki, Characterization of airborne particulates and associated trace metals deposited on tree bark by ICP–OES, ICP–MS, SEM–EDX and laser ablation ICP–MS, Atmos. Environ. 40 (2006) 2626–2634.
[6] WHO (World Health Organization), Air Quality Guidelines for Europe, second ed., WHO Regional Publications, Regional Office for Europe, Copenhagen, Denmark, 2000.
[7] A. Banerjee, Heavy metal levels and solid phase speciation in street dusts of Delhi, India, Environ. Pollut. 123 (2003) 95–105.
[8] M. Imperato, P. Adamo, D. Naimo, M. Arienzo, D. Stanzione, P. Violante, Spatial distribution of heavy metals in urban soils of Naples city (Italy), Environ. Pollut. 124 (2003) 247–256.
[9] A.G. Allen, E. Nemitz, J.P. Shi, R.M. Harrison, J.C. Greenwood, Size distributions of trace metals in atmospheric aerosols in the United Kingdom, Atmos. Environ. 35 (2001) 4581–4591.
[10] K.V. Desboeufs, A. Sofitikis, R. Losno, J.L. Colin, P. Ausset, Dissolution and solubility of trace metals from natural and anthropogenic aerosol particulate matter, Chemosphere 58 (2005) 195–203.
[11] G. Shi, Z. Chen, C. Bi, Y. Li, J. Teng, L. Wang, S. Xu, Comprehensive assessment of toxic metals in urban and suburban street deposited sediments (SDSs) in the biggest metropolitan area of China, Environ. Pollut. 158 (2010) 694–703.
[12] P.A. de P. Pereira, W.A. Lopesa, L.S. Carvalhoa, G.O. da Rochab, N. de C. Bahiaa, J. Loyola, S.L. Quiterio, V. Escaleira, G. Arbilla, J.B. de Andrade, Atmospheric concentrations and dry deposition fluxes of particulate trace metals in Salvador, Bahia, Brazil, Atmos. Environ. 41 (2007) 7837–7850.
[13] D.J. Swaine, Why trace elements are important, Fuel Process. Technol. 65 (2000) 21–33.
[14] Y. Gao, E.D. Nelson, M.P. Field, Q. Ding, H. Li, R.M. Sherrell, C.L. Gigliotti, D.A. Van Ry, T.R. Glenn, S.J. Eisenreich, Characterization of atmospheric trace elements on PM2.5 particulate matter over the New York–New Jersey harbor estuary, Atmos. Environ. 36 (2002) 1077–1086.
[15] G.G. Pyle, S.M. Swanson, D.M. Lehmkuhl, Toxicity of uranium mine receiving waters to caged fathead minnows, *Pimephales promelas*, Ecotoxicol. Environ. Saf. 48 (2001) 202–214.
[16] J. Shu, J.A. Dearing, A.P. Morse, L. Yu, N. Yuan, Determining the sources of atmospheric particles in Shanghai, China, from magnetic and geochemical properties, Atmos. Environ. 35 (2001) 2615–2625.
[17] G.C. Fang, W.J. Huang, J.C. Chen, J.H. Huang, Y.L. Huang, Study of ambient air particle-bound As(p) and Hg(p) in dry deposition, total suspended particulates (TSP) and seasonal variations in Central Taiwan, Environ. Forensics 12 (2011) 7–13.
[18] C.A.I. Pope, D.W. Dockery, J. Schwartz, Review of epidemiological evidence of health effects of particulate air pollution, Inhalat. Toxicol. 7 (1995) 1–18.
[19] B. Brunekreef, S.T. Holgate, Air pollution and health, Lancet 360 (2002) 1233–1242.
[20] C.A. Pope, D.W. Dockery, Epidemiology of particle effects, in: S.T. Holgate, J.M. Samet, H.S. Koren, R.L. Maynard (Eds.), Air Pollution and Health, Academic Press, 1999, pp. 673–706.
[21] K.T. Donaldson, S. Mill, W. MacNee, S. Robinson, D. Newby, Role of inflammation in cardiopulmonary health effects of PM, Toxicol. Appl. Pharmacol. 207 (2) (2005) 483–488.
[22] A. Baklanov, J.H. Sorensen, Parameterisation of radionuclide deposition in atmosphere long-range transport modeling, Phys. Chem. Earth 26 (2001) 787–799.
[23] G.C. Fang, Y.S. Wu, S.H. Huang, J.Y. Ran, Size distributions of ambient air particles and enrichment factor analyses of metallic elements at Taichung Harbor near the Taiwan Strait, Atmos. Res. 81 (2006) 320–333.
[24] N. Basu, A.M. Scheuhammer, C. Sonne, R.J. Letcher, E.W. Born, R. Dietz, Is dietary mercury of neurotoxicological concern to wild polar bears, Environ. Toxicol. Chem. 28 (2009) 133–140.
[25] E. Näslund, L. Thaning, On the settling velocity in a nonstationary atmosphere, Aerosol Sci. Technol. 12 (1991) 247–256.
[26] Y.P. Fang Kenneth, Measurement and modeling of atmospheric coarse particle deposition to a flat plate, Ph.D. Thesis, Illinois Institute of Technology, Chicago, IL, 1989.
[27] P. Zannetti, Air Pollution Modeling: Theories, Computational Methods, and Available Software, 1990, 444 pp., ISBN 1853121002.
[28] T. Okuda, M. Katsuno, D. Naoi, S. Nakao, S. Tanaka, K. He, Y. Ma, Y. Lei, Y. Jia, Trends in hazardous trace metal concentrations in aerosols collected in Beijing, China from 2001 to 2006, Chemosphere 72 (2008) 917–924.
[29] S.L. Celine, X.D. Lee, G.Z. Li, J. Li, A.J. Ding, T. Wang, Heavy metals and Pb isotopic composition of aerosols in urban and suburban areas of Hong Kong and Guangzhou, South China—evidence of the long-range transport of air contaminants, Atmos. Environ. 41 (2007) 432–447.
[30] F. Var, Y. Narita, S. Tanaka, The concentration, trend and seasonal variation of metals in the atmosphere in 16 Japanese cities shown by the results of National Air Surveillance Network (NASN) from 1974 to 1996, Atmos. Environ. 34 (2000) 2755–2770.
[31] P.D. P.D.Hien, N.T. Binh, Y. Truong, N.T. Ngo, L.N. Sieu, Comparative receptor modelling study of TSP, PM2 and PM2-10 in Ho Chi Minh City, Atmos. Environ. 35 (2001) 2669–2678.
[32] G.C. Fang, C.N. Chang, C.C. Chu, Y.S. Wu, P.P.C. Fu, I.L. Yang, M.H. Che, Characterization of particulate, metallic elements of TSP, PM2.5 and PM2.5–10 aerosols at a farm sampling site in Taiwan, Taichung, Sci. Total Environ. 308 (2003) 157–166.
[33] K.H. Kim, J.H. Lee, M.S. Jang, Metals in airborne particulate matter from the first and second industrial complex area of Taejon city, Korea, Environ. Pollut. 118 (2002) 41–51.
[34] P.S. Khillare, S. Balachandran, B.R. Meena, Spatial and temporal variation of heavy metals in atmospheric aerosols of Delhi, Environ. Monit. Assess. 90 (2004) 1–21.
[35] Environmental Analysis Laboratory EPA. Executive Yuan, R.O.C. (Taiwan EPA).

[36] E. Bruggemann, H. Gerwig, Th Gnauk, K. Muller, H. Herrmann, Influence of seasons, air mass origin and day of the week on size-segregated chemical composition of aerosol particles at a kerbside, Atmos. Environ. 43 (2009) 2456–2463.
[37] E. von Schneidemesser, E.A. Stone, T.A. Quraishi, M.M. Shafer, J.J. Schauer, Toxic metals in the atmosphere in Lahore, Pakistan, Sci. Total Environ. 408 (2010) 1640–1648.
[38] G.C. Fang, S.C. Chang, Atmospheric particulate (PM_{10} and $PM_{2.5}$) mass concentration and seasonal variation study in the Taiwan area during 2000–2008, Atmos. Res. 98 (2010) 368–377.
[39] B.K. Lee, N.T. Hieu, Seasonal variation and sources of heavy metals in atmospheric aerosols in a residential area of Ulsan, Korea, Aerosol Air Qual. Res. 11 (2011) 679–688.